The Increase in the Center of Mass Momentum of a System due to Fictitious Forces within a Rectilinear Accelerated Three-Body System

Paul R. Mesler

Independent Researcher

Provo, Utah

Email: rst44e@gmail.com

Date: May 2026

Keywords: Euler's first law, center of mass momentum, principle of equivalence, geodesic equation, Christoffel symbols, fictitious forces

Abstract

We report the results of an experiment where after 30 test trials the mean value of known external friction impulses acting on a three-body system accounted for only ~ 8.2 per cent (standard deviation .037 and standard error .0068) of the increase in the final momentum of the system, leaving a ~ 91.8 per cent discrepancy due to an unknown impulse. In this paper we propose an explanation for this impulse that accounts for this discrepancy. The three-body system consisted of two spheres, constrained to roll around quarter-circle barriers attached to a third body. As the spheres rounded the curves, centripetal contact forces acted on the spheres while equal and opposite centrifugal reactive contact forces acted on the inner walls of the curved barriers. These centrifugal reactive contact forces caused the system to accelerate, inducing fictitious body forces on the spheres that increased their orbital angular speed. We cite Einstein's principle of equivalence to explain this increase in speed.

1. Introduction

This experiment is based on the results of a prior experiment we performed. In this preliminary experiment a rotating body (rotator) with a vertical shaft was inserted at one end into a bearing assembly that was embedded in a platform. This platform could slide along bearings attached to the platform within the grooves of a linear track. One Pasco accelerometer was attached to the platform and another accelerometer to the rotator. The platform was initially butted against a barrier so that it could not move in the negative y-direction. A counter-clockwise rotation was imparted to the rotator when it was approximately at the 270 degrees position. When the rotator passed the 0 degrees point, the platform accelerated in the positive y-direction. The accelerometer reported the data via Blue Tooth to a Pasco program on a computer that plotted the graph of the acceleration.

The data graphed a sinusoidal wave with zero acceleration for the platform at the zero degrees point, a maximum acceleration at the 90 degrees point, and zero acceleration at the 180 degrees point, followed by a maximum acceleration at the 270 degrees point and so on. When the rotator passed the 90 degrees and the 270 degrees point as the system continued to accelerate and de-accelerate, the accelerometer on the rotator showed an increase in its orbital angular speed.

Since the same increase in orbital angular speed was observed in both the accelerated frame and in our inertial frame, this led us to question if it is possible that with respect to our inertial laboratory frame, could there be an increase in the center of mass momentum of a linearly-accelerated system relating to this frame invariant increase in angular speed? This was the motivation for the experiment reported in this paper.

2. Materials and Methods

Figure 1

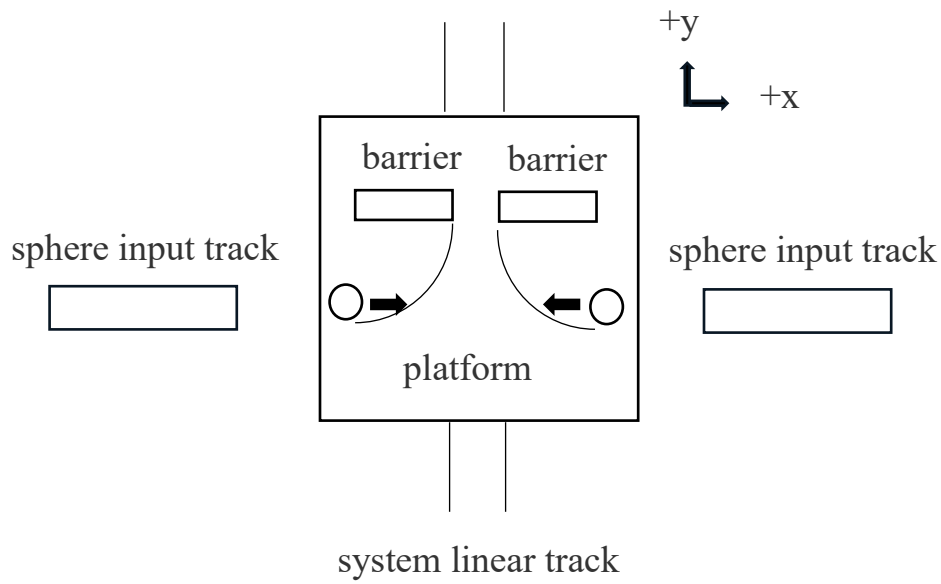

In this experiment we attached a platform to the top of a Pasco Smart Cart which was free to travel on top of an aluminum linear track horizontal to the earth with one degree of freedom as shown above in the top-down view of Figure 1. Attached to the surface of the platform were two quarter-circle curves and two barriers. The platform, curves, barriers, and Pasco Smart Cart taken together constituted the mass designated as m_2. Two spheres of equal mass, designated by m_1, entered the surface of the platform simultaneously, rolling along the x-axis with equal initial velocities, designated by v_i. The two spheres were constrained to travel around these quarter-circle barriers. One sphere rounded a curve on the left and traveled counter-clockwise from 270 degrees to 0 degrees and the other sphere rounded a curve on the right and traveled clockwise from 270 degrees to 180 degrees.

As the spheres rounded their curves, centrifugal reactive contact forces, opposite the equal and opposite centripetal contact forces on the spheres, acted on the curves and caused the platform-cart assembly to accelerate in the negative y-direction. Immediately, after rounding and existing the curves, both spheres made inelastic collisions with the barriers in the positive y-

direction, causing the spheres-platform system to acquire a post collision momentum in the positive y-direction. The time and velocity values of the system were communicated by Blue Tooth from the Pasco Smart Cart to a laptop.

It was crucial in this experiment that the two spheres entered the platform with the same speed and that they entered the surface of the platform simultaneously. This was necessary in order to cancel out any forces acting on the platform along the x-axis. We were only interested in forces that acted along the y-axis. And it was important that the two spheres enter the platform simultaneously at the same speed else the cart could twist completely off the track.

Each sphere had a m_1 mass of .5330 kg ± .0001 kg. The m_2 mass was .4492 kg ± .0001 kg. A digital level with a resolution of .1 degrees was used to check if the linear track was level with respect to the horizontal x and y-axes. Each barriers the spheres collided into contained neodymium magnets to prevent bounce back after the collision of the spheres. The mass of each magnet was 14.7 ± .1 g.

The core of this experiment was to measure the impact of friction impulses on the system to see if they accounted for all of the final momentum of the system. When the platform rolled backwards in the negative y-direction as the spheres rounded their curves, external friction impulses acted on the system in the positive y-direction. The friction force for each trial was determined by dividing the post collision momentum of the system by the time it took the system to come to a stop. The friction impulse was calculated by multiplying the time the cart moved in the negative y-direction times this friction force.

It was not necessary to determine the rolling friction between the spheres and platform's surface and curved barriers since these were internal force pairs that would have no impact on

the center of mass of the system. Air friction effects were also ignored since the speeds of the cart and spheres were small enough that any air friction drag effects would have negligible impact on the outcome.

Because the experiment was built of low-density PLA fiber, the system was susceptible to high frequency mechanical vibrations and noise which clouded the interpretation of the final post collision velocity of the spheres and time increment readings and often required a conservative interpretation of the data. The sample rate of the Pasco Smart Cart used in the experiment was 50 HZ.

In future replications of the experiment, it is recommended that higher density materials be used to dampen the mechanical noise as long as the ratio of the total mass of the spheres to the mass of the platform be at least 2:1. Initial velocity of the spheres should be as high as possible as the acceleration of the system is proportional to this speed.

3. Results

Table 1. Data summary of 30 Test Trials

Initial Sphere Velocity	Back Time	Friction Force	Friction Impulse	Post Collision Velocity	Post Collision Momentum	Impulse to Momentum Ratio
m/s	s	N	N · s	m/s	Kg · m/s	
0.65	0.154	0.0249	0.0038	0.047	0.071	0.05

0.65	0.116	0.0704	0.0082	0.053	0.080	0.10
0.65	0.171	0.0131	0.0022	0.025	0.038	0.06
0.66	0.148	0.0144	0.0021	0.028	0.042	0.05
0.65	0.141	0.0281	0.0040	0.033	0.050	0.08
0.65	0.192	0.0309	0.0059	0.051	0.077	0.08
0.66	0.264	0.0360	0.0095	0.034	0.052	0.18
0.65	0.137	0.0492	0.0067	0.077	0.12	0.06
0.65	0.186	0.0370	0.0069	0.044	0.067	0.10
0.65	0.132	0.0292	0.0039	0.032	0.048	0.08
0.65	0.135	0.0206	0.0028	0.035	0.053	0.05
0.66	0.155	0.0498	0.0077	0.047	0.071	0.11
0.66	0.164	0.0489	0.0080	0.06	0.091	0.088
0.66	0.2	0.0323	0.0065	0.046	0.070	0.09
0.67	0.212	0.0463	0.0098	0.063	0.095	0.10
0.65	0.136	0.0374	0.0051	0.039	0.059	0.09
0.66	0.195	0.0543	0.0106	0.033	0.050	0.21
0.67	0.195	0.0150	0.0029	0.023	0.035	0.08
0.67	0.132	0.0349	0.0046	0.052	0.08	0.06
0.65	0.186	0.0410	0.0076	0.059	0.089	0.09
0.66	0.133	0.0172	0.0023	0.036	0.055	0.04
0.66	0.19	0.0175	0.0033	0.045	0.068	0.05
0.65	0.149	0.0379	0.0056	0.037	0.06	0.10
0.65	0.198	0.0147	0.0029	0.028	0.042	0.07

0.65	0.152	0.0388	0.0059	0.042	0.06	0.09
0.66	0.127	0.0147	0.0019	0.032	0.048	0.04
0.66	0.2	0.0219	0.0044	0.028	0.04	0.10
0.66	0.19	0.0172	0.0033	0.037	0.056	0.06
0.66	0.21	0.0124	0.0026	0.027	0.041	0.06
0.73	0.137	0.0249	0.0034	0.051	0.08	0.04

Statistical summary of impulse to momentum ratio for 30 test trials

Mean .082

Std Dev .037

Std Error .0068

Constants Used in Table 1 Calculations

Total Mass (kg) 1.5152 ± 0.0002 kg

The back time was the time the platform moved backwards from its initial at rest state to the time it attained its maximum value. Post collision velocity was the maximum velocity of the platform right after the collision of the two spheres with their barriers.

4. Discussion

The principle of equivalence (Einstein, 1916) states not only is there an equivalence of electromagnetic behavior between a gravitational field and an accelerated system but also includes the equivalence of all mechanical behavior. What happens to a sphere rolling around a quarter circle curve in a gravitational field is what happens to a sphere in an accelerated system.

As the platform accelerated in the negative y-direction due to the centrifugal reactive contact forces acting on the inner walls of the curved barriers, a local gravitational field occurred with respect to the accelerated platform frame. Within this non-flat metric space, the geodesic equation of general relativity defined the geodesic paths of the spheres due to the fictitious body forces acting in the positive y-direction, encoded in the Christoffel symbols $\Gamma^{\mu}_{\alpha\beta}$ of the geodesic equation below:

$$\frac{d^2x^{\mu}}{d\tau^2} + \Gamma^{\mu}_{\alpha\beta}\frac{x^{\alpha}}{d\tau}\frac{x^{\beta}}{d\tau} = 0$$

Applying this equation within the frame of the accelerating platform would yield an increase in the speeds of the spheres as they "fall" downward in their gravitational field in the positive y-direction. Because of the complex, non-constant, sinusoidal nature of the system's acceleration, computer numerical approximation techniques would be required in applying this equation to solve for the final speeds of the spheres. The result will show an increase in the final orbital angular speed which is invariant with respect to both the accelerated frame and our laboratory inertial frame.

We can isolate *when* the unknown impulse occurs reported in this paper. If this experiment were conducted in a near frictionless environment, such as in interstellar space, the additional impulse could not occur while the spheres were propelled and travelled along the x-axis. Neither could the missing impulse occur after the spheres exited the curves because during these times, the center of mass momentum of the system is in equilibrium with respect to the y-axis. Hence, this additional impulse must occur during the time the spheres round their curves. This points to fictitious body forces as being the cause of the additional impulse.

Within a rectilinear accelerated system, fictitious body forces that act on bodies do not comply with Newton's third law. They are forces that do not arise from physical contact with another body, thus, there is no equal and opposite force to the fictitious force acting on the curves of the platform. *Fictitious body forces arise from the interaction of the body with the local curved spacetime metric of the accelerating platform and not through physical contact with another body.*

This "one force" action of the fictitious forces is an essential requirement in inducing a change in the center of mass momentum of a system. If there were an equal and opposite effect on the walls of the curve, there would be no impact on the center of mass momentum. The two equal and opposite forces would cancel.

Thus, first principles of classical mechanics predicts that if a *single* force acts on *one* body of a multi-body system which changes the momentum of that body, this would equate to a change in momentum of the center of mass of the whole system. This is the crux of our principle of equivalence explanation that accounts for the ~ 91.8 per cent impulse discrepancy for the final center of mass momentum of the system in the experiment.

5. Conclusion

Einstein's principle of equivalence and the application of the geodesic equation is the foundation for the kinetic explanation of the impulse discrepancy measured in this experiment. In addition, it follows that any increase in the center of mass momentum of a system by an external force impulse predicted by Euler's first law, implies the same force has done work *on* the system to increase its kinetic energy which follows from the work-energy theorem and the first law of thermodynamics.

It is recommended that further experiments be conducted in a near zero friction environment on an air track or within a plane in a zero-g dive or by a CubeSat in space where the effects of external friction forces would be reduced significantly. Appendix A contains a set of equations that can be used for further testing and confirmation of the effect in near frictionless environments.

Appendix A

This appendix presents a set of five equations for predicting the motions of a more complicated system. These equations apply in idealized environments where external friction impulses or other external impulses are nearly eliminated such as in the environment of inter-stellar space. In this more elaborate system, the total mass m is the sum of the masses of the spheres, the platform, and all attachments to the platform.

We need to define what a cycle N means. In this system two spheres are propelled by the release of two compressed springs, afterwards the spheres enter and round quarter-circle curves, then have elastic collisions with elastic barriers after existing the curves, bounce back, and then round the curves again in the opposite direction, returning to their initial positions, and finally resting against the two recompressed springs. This is defined as one cycle N. We denote a virtual external impulse J_{virtual}, defined by measuring the change in momentum of the system after one cycle.

The compressed springs which propel the spheres store elastic potential energy (epe) which is a scalar or invariant quantity that does not depend on the velocity of the system. Denoting the total number of springs as n and the energy per compressed spring as epe, the cumulative energy applied to the spheres after N cycles is:

$$E_{\text{cumulative}} = N\, n\, epe \qquad (A1)$$

The cumulative final velocity of the system, with external impulse J_{virtual}, after N cycles equate to:

$$v_{f\ \text{system}} = \frac{N\, J_{\text{virtual}}}{m} \qquad (A2)$$

Substituting $v_{f\ \text{system}}$ into the formula for kinetic energy yields:

$$KE_{\text{final}} = \frac{(N\, J_{\text{virtual}})^2}{2m} \qquad (A3)$$

The cycle N at which KE_{final} equals $E_{\text{cumulative}}$ is determined by setting Equation (A1) equal to Equation (A3), then solving for N, giving us:

$$N = \frac{2\, m\, epe}{J_{virtual}^2} \qquad (A4)$$

For other engineering applications and insight, it is useful to graph both Equation (A1) and Equation (A3) to visually see their relationship with N as the x-axis and energy as the y-axis.

The value for m can easily be predetermined by direct measurement. The value for epe can be calculated knowing the spring constant and the degree of compression. The virtual impulse J_{virtual} is determined experimentally by activating a single cycle when the system is at rest and measuring the system's final velocity v_f, giving us the virtual impulse as:

$$J_{\text{virtual}} = m\, v_f \qquad \text{(A5)}$$

Declaration of AI Use

During the preparation of this work, the author used generative AI to assist with academic formatting and recommendations on scientific language used in the paper. The author reviewed and edited the content and takes full responsibility for the publication.

Acknowledgments

The author identifies as an independent researcher and received no institutional support for this study. All experimental trials were conducted privately.

Data Availability

Pasco data relating to the experiments is available for review upon request.

References

Einstein, A. (1916). The Foundation of the General Theory of Relativity (*Die Grundlage der allgemeinen Relativitätstheorie*). *Annalen der Physik*, 49(7), 769–822. doi.org